Supporting Information

Computational photon counting using multi-threshold peak detection for fast fluorescence lifetime imaging microscopy

Janet E. Sorrells[a,b], Rishyashring R. Iyer[b,c], Lingxiao Yang[b,c], Elisabeth M. Martin[a,b], Geng Wang[b], Haohua Tu[b,c], Marina Marjanovic[a,b], Stephen A. Boppart[a,b,c,d,e*]

[a]Department of Bioengineering, University of Illinois at Urbana-Champaign, Urbana, IL 61801, United States

[b]Beckman Institute for Advanced Science and Technology, University of Illinois at Urbana-Champaign, Urbana, IL 61801, United States

[c]Department of Electrical and Computer Engineering, University of Illinois at Urbana-Champaign, Urbana, IL 61801, United States

[d]Cancer Center at Illinois, Urbana, IL 61801, United States

[e]Carle Illinois College of Medicine, University of Illinois at Urbana-Champaign, Urbana, IL 61801, United States

*boppart@illinois.edu

SUPPORTING INFORMATION:

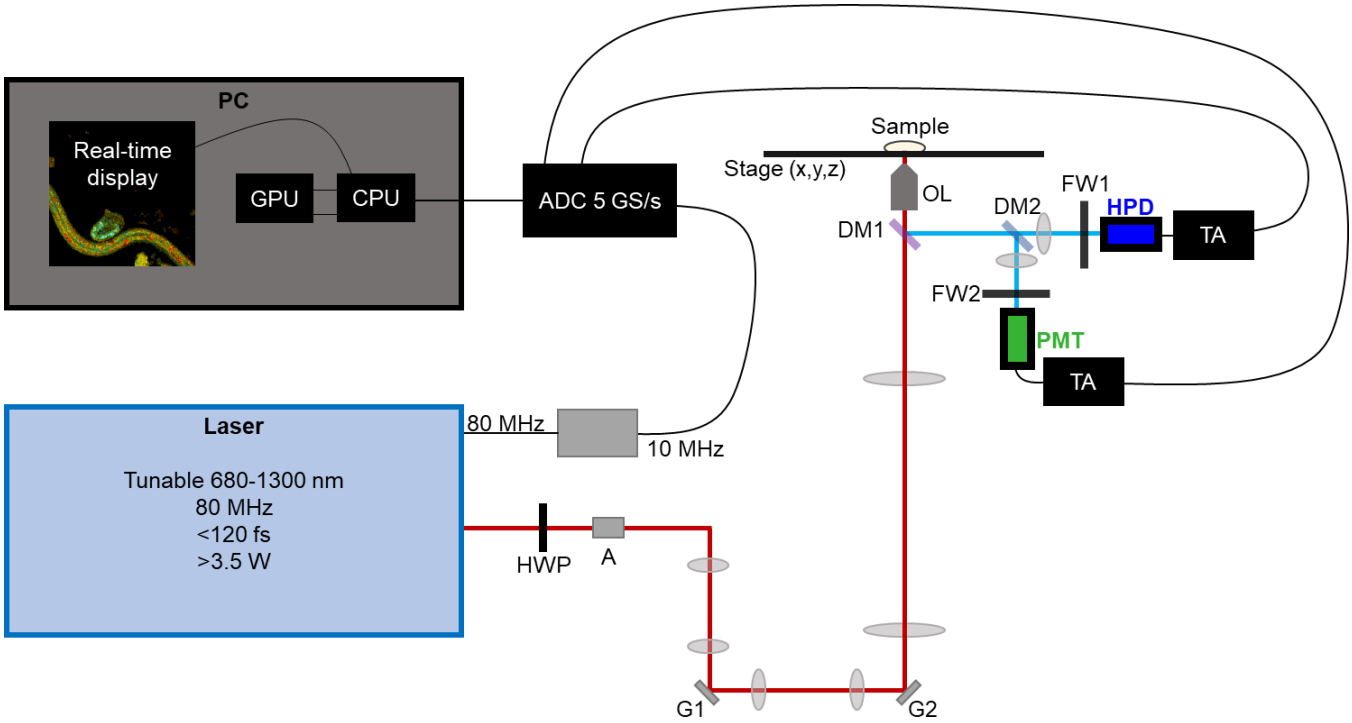

Figure S1. Custom two-photon FLIM setup for implementing single- and multi-photon peak event detection (SPEED) using a pulsed laser at 80 MHz and direct digitization of detector output. The repetition rate of the laser was downsampled to a 10 MHz clock to synchronize the ADC and DAQ.[S1] Two galvanometer mirrors are used to scan the beam on the sample to sequentially excite each pixel. The sample can be translated in three dimensions using the stage to choose the optimal location for imaging or take mosaics. Emitted fluorescence below 665 nm is directed by a dichroic mirror towards the detectors. A removable dichroic mirror box is used to direct signal to either the HPD or the PMT, both of which are equipped with filter wheels with different bandpass filters for selection of spectral bands. Signal from the detectors is amplified by a 20 dB, 2.5 GHz bandwidth transimpedance amplifier, and then digitized at 5 GS/s. Raw data can be saved directly for system characterization analysis, and/or processed on the GPU for real-time display and saving of processed data. HWP, half wave plate; A, attenuator; G, galvo; DM, dichroic mirror; OL, objective lens; FW, filter wheel; HPD, hybrid photodetector; PMT, photomultiplier tube; TA, transimpedance amplifier; ADC, analog-to-digital converter; CPU, central processing unit; GPU, graphics processing unit.

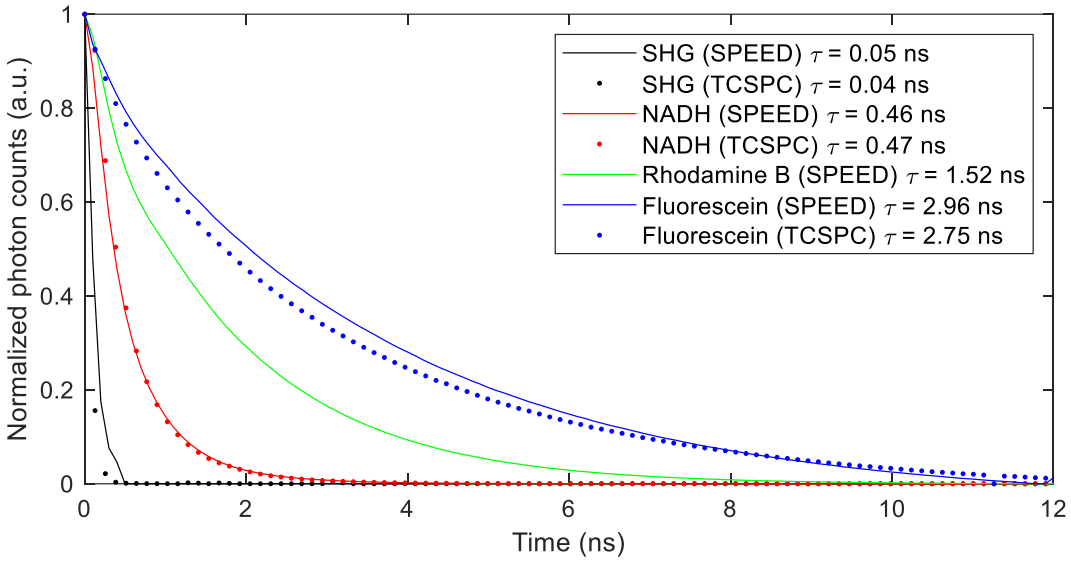

Figure S2. Fluorescence decay curves of fluorescent standards using single- and multi-photon peak event detection (SPEED) and TCSPC. Data was collected form freshly prepared standards on different days on different systems; data using SPEED was collected on the system presented in Fig. S1 using the HPD and data using TCSPC was collected using the NADH fluorescence channel of a different custom two-photon FLIM microscope with a TCSPC system.[S2] This TCSPC system has a bandpass filter for 451±53 nm (designed for NADH), which is not ideal for collection of Fluorescein and inhibited collection of Rhodamine B fluorescence. This spectral difference may be why Fluorescein fluorescence lifetime using TCSPC was lower than using SPEED, and lower than previously reported by other sources closer to 3.6 ns.[S3] Solutions were prepared as: SHG from urea crystal, NADH 5 mM in 1 M 7.4 pH HEPES buffer, Rhodamine B 1 mg/mL in distilled water, Fluorescein 1 mg/mL in 100% ethanol. All photon rates for SPEED were between 1% and 100% to ensure accurate estimation and between 0.5% and 5% for TCSPC.

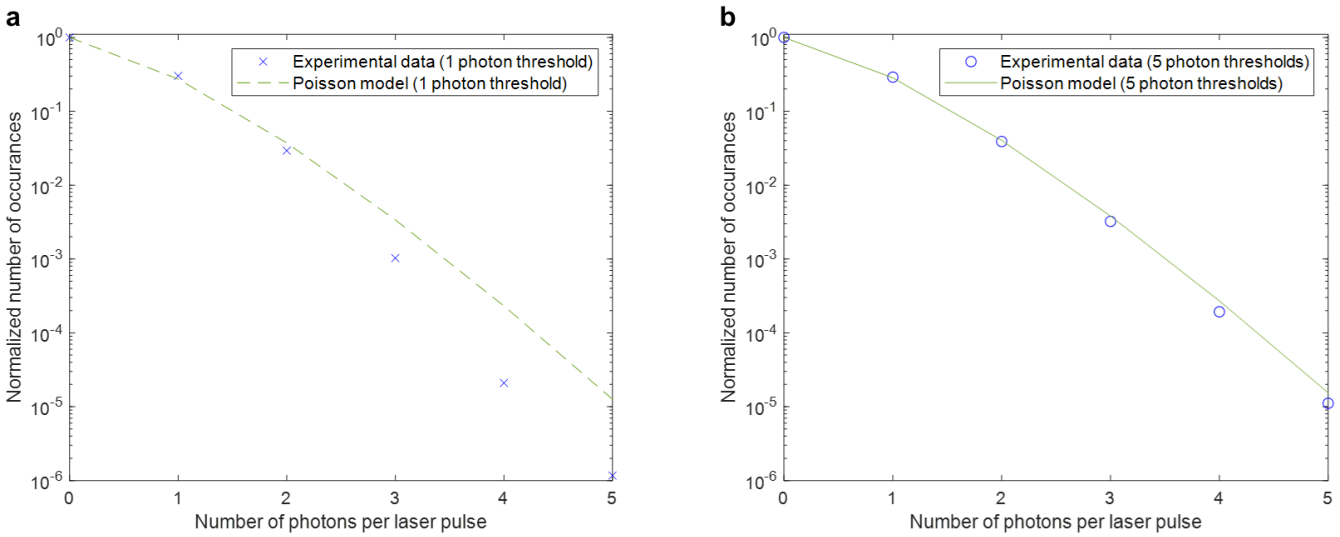

Figure S3. Photon counting histograms using either one (a) or five (b) photon thresholds and fit to Poisson model. Data is from one frame of two-photon fluorescence of a 10 mM NADH solution. Photon counting histograms are often using for analysis of fluorescence data.[S4] Using five photon thresholds provided a better fit to the Poisson model, indicating a more accurate way to count photons. Note that nonuniformity of the illumination over the frame may be a cause of error.

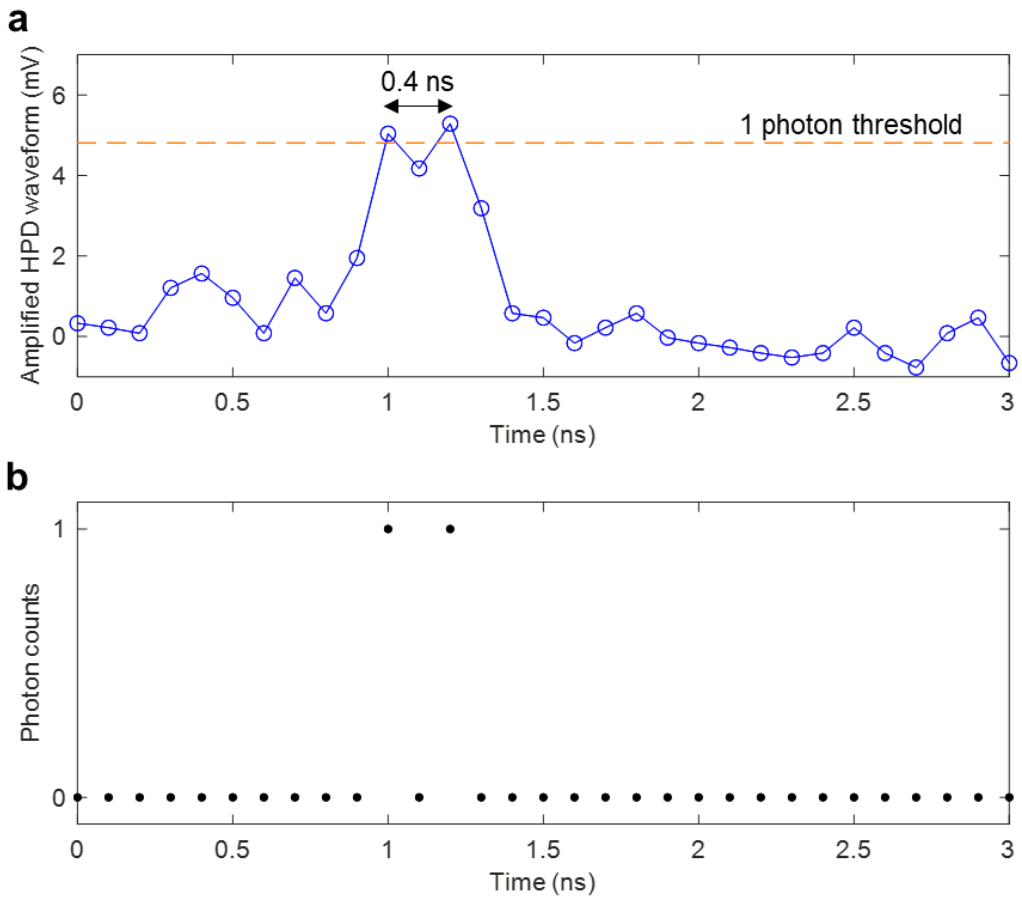

Figure S4. Example dead time verification using hybrid photodetector (HPD) and high bandwidth amplification (2.5 GHz) and digitization (5 GS/s). (a) Directly digitized HPD waveform (blue, in mV) for two consecutive photons arriving at the detector, creating two distinct peaks in the data that are both above the 1 photon peak threshold. (b) Corresponding photon counts from the data shown in (a).

Supplementary Note 1: Temporal alignment of digitized fluorescence signal with laser clock. Digitization of raw data is synchronized to the laser clock, however the relative temporal location of the laser pulse is unknown in digitized data and must be inferred from the data. In other words, the relative time between photon counts (i.e. 3 ns) is clear from digitized data, but the time between those photon counts and the laser excitation pulse is unknown. In order to determine the likely temporal alignment with the laser pulse, the resultant fluorescence decays can be examined, and it can be assumed that the maximum value within the decay curve is aligned with the excitation pulse. For example, in Figure 2c, data from one pixel is summed into 25 ns segments to represent two laser periods. The maximum value falls around 2.5 ns, so it is likely that this aligns with the laser excitation. Data is then circularly shifted so that the maximum value falls at time t = 0.

Our previous implementation of computational photon counting[S5] used the maximum value of the resultant fluorescence decay from each pixel to shift each pixel individually. In this implementation, we examined whether using more data to create the resultant decay that is used to determine the relative temporal shift would improve capabilities. Since each line of data of the image is digitized continuously, we used the resultant decay from summing together all 25 ns segments within one line of data and shifting the entire line based on that maximum value, and compared it to using our previous method of shifting each pixel individually. Especially for lower concentrations of NAD(P)H, using an entire line of data (containing approximately 512 times more photons for a 512 × 512 image) produced better results (Figure S5).

Using more data to infer temporal alignment provides better results since it provides more context. For example, for a very low intensity image, one pixel of the image may receive only one photon. Using the pixel-shifting scheme, this one photon would be the maximum and would be aligned with time t = 0 ns. If this happens to many pixels within the image, the resultant decay would be significantly artificially biased towards sooner-arriving photonics, and the calculated fluorescence lifetime would be artificially too low (Figure S5d). However, if an entire line of data is summed together, even if the average number of photons per pixel is slightly less than one, the resultant decay used to determine the temporal shift would still contain hundreds of photons, and thus provide a proper fluorescence decay curve to more accurately determine temporal alignment of each pixel, and thus provide more accurate fluorescence lifetime values.

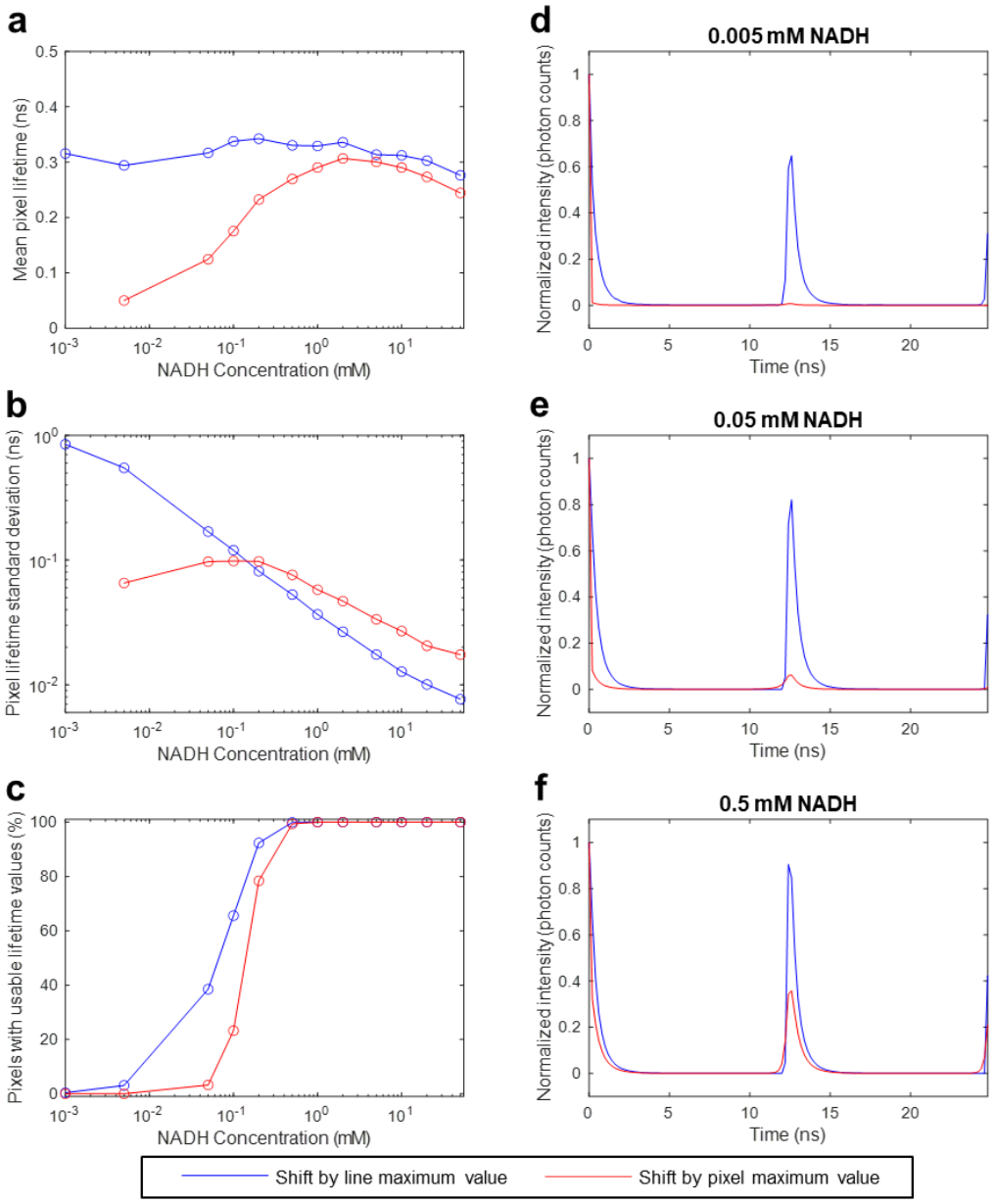

Figure S5. The effect of aligning and shifting the maximum value of each line (blue) or each pixel (red) in order to infer temporal alignment with the laser excitation pulse. This can be done by examining the resultant fluorescence decay, and assigning the maximum value of a fluorescence decay (where the fluorescence decay used is the sum of all photons collected in either each line (blue) or each pixel (red)) as a point that is temporally aligned with the laser pulse. Photon counts are cut into 25 ns segments that are summed together to form the resultant decay curves (Figure 2c); the effect of using interleaved sampling at 5 GS/s leads to two decay curves in each 25 ns segment. (a) Mean pixel fluorescence lifetime, (b) pixel fluorescence lifetime standard deviation, and (c) percentage of pixels with usable lifetime values (with usable defined as any fluorescence lifetime between 0 and 12.5 ns) when using the maximum value in each line or each pixel to shift the data. When the signal-to-noise ratio is low, for example (d) for 0.005 mM NADH low fluorescence lifetimes are artificially biased low. As signal increases, using the fluorescence decays determined using pixel-shifting approach those using line shifting (e,f).

Supplementary Note 2: Mammalian cell culture and treatment. A human epithelial breast adenocarcinoma cell line (MCF7, ATCC HTB-22) was maintained in EMEM media supplemented with 10% fetal bovine serum (Hyclone Laboratories), 1% penicillin streptomycin antibiotic (Thermo Fisher Scientific), 4 mM glutamine (Thermo Fisher Scientific), and 5 μg/mL insulin (Sigma-Aldrich), plated on poly-d-lysine coated imaging dishes (P35GC-0-10-C, MatTek) and left to settle for 24 hours. During imaging, a 20 μM stock solution of Staurosporine (a known inducer of apoptosis that has previously been shown to cause an increase in fluorescence intensity and lifetime of NAD(P)H in cells[S5,S6]) in DMSO was added to the dish with cells containing 2 mL of media for a final concentration of 1 μM.

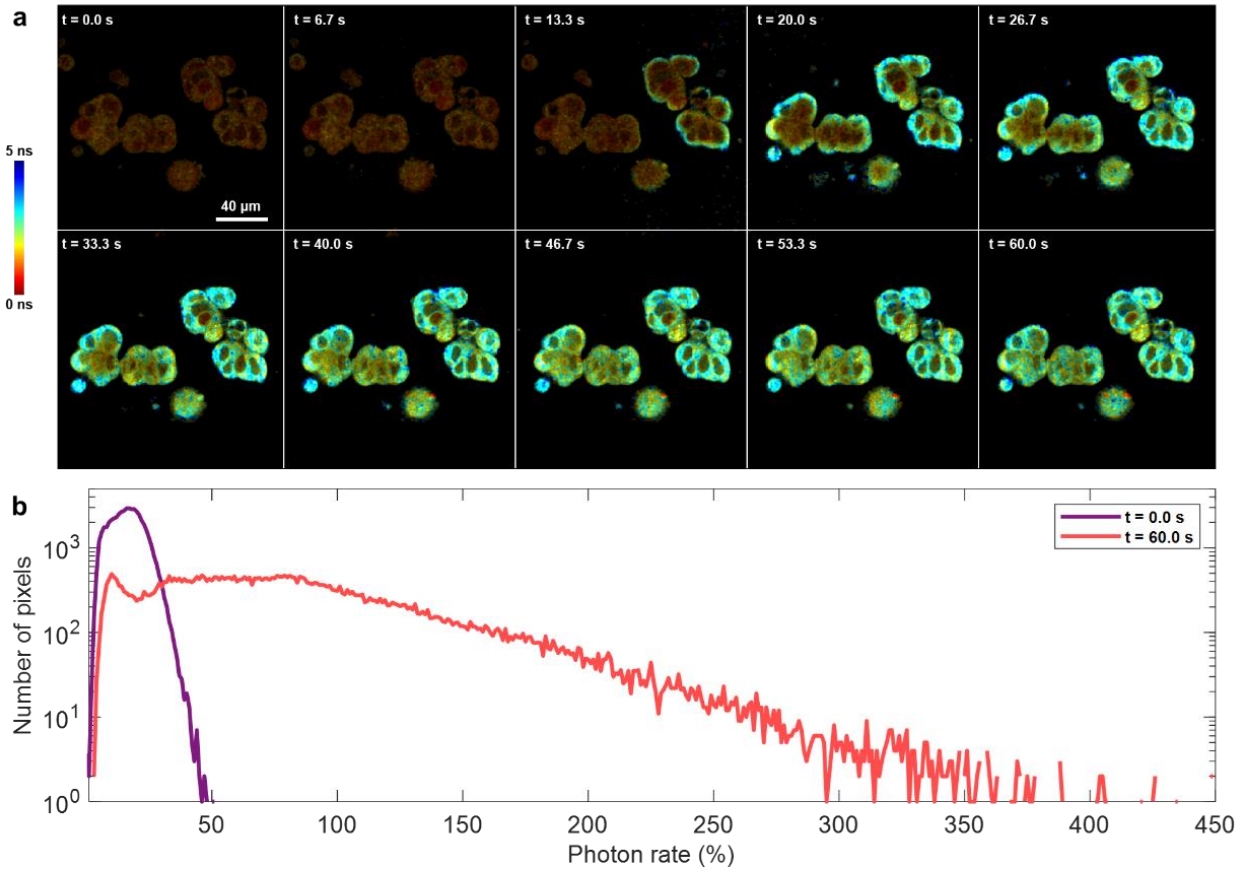

Figure S6. Apoptosis dynamics in human breast cancer cells by addition of 1 μM Staurosporine at t = 0.0 s. (a) Fluorescence lifetime overlaid on intensity of human breast cancer cells over one minute. (b) Histogram of nonzero photon rates within pixels of the whole image at t = 0.0 s (purple) and t = 60.0 s (red).

SUPPORTING REFERENCES

S1. Iyer, R.R.; Sorrells, J.E.; Yang, L.; Chaney, E.J.; Spillman Jr., D.R.; Tibble, B.E.; Renteria, C.A.; Tu, H.; Žurauskas, M.; Marjanovic, M.; Boppart, S.A. Label-free metabolic and structural profiling of dynamic biological samples using multimodal optical microscopy with sensorless adaptive optics. Sci. Rep. **2022**, *12*, 3438.

S2. Lee, J.H.; Rico-Jimenez, J.J.; Zhang, C.; Alex, A.; Chaney, E.J.; Barkalifa, R.; Spillman, D.R.; Marjanovic, M.; Arp, Z.; Hood, S.R.; Boppart, S.A. Simultaneous label-free autofluorescence and multi-harmonic imaging reveals *in vivo* structural and metabolic changes in murine skin. Biomed. Opt. Express **2019**, *10(10)*, 5431-5444.

S3. Kristoffersen, A.S.; Erga, S.R.; Hamre, B.; Frette, Ø. Testing fluorescence lifetime standards using two-photon excitation and time-domain instrumentation: Fluorescein, Quinine Sulfate, and Green Fluorescent Protein. J. Fluoresc. **2018**, *28*, 1065-1073.

S4. Chen, Y.; Müller, J.D.; So, P.T.C.; Gratton, E. The photon counting histogram in fluorescence fluctuation spectroscopy. Biophys. J. **1999**, *77(1)*, 553-567.

S5. Sorrells, J.E.; Iyer, R.R.; Yang, L.; Chaney, E.J.; Marjanovic, M.; Tu, H.; Boppart, S.A. Single-photon peak event detection (SPEED): a computational method for fast photon counting in fluorescence lifetime imaging microscopy. Opt. Express **2021**, *29(23)*, 37759-37775.

S6. Bower, A. J.; Sorrells, J.E.; Li, J.; Marjanovic, M.; Barkalifa, R.; Boppart, S.A. Tracking metabolic dynamics of apoptosis with high-speed two-photon fluorescence lifetime imaging microscopy. Biomed. Opt. Express **2019**, *10(12)*, 6408-6421.